ARTICLE

Line-profile Analysis of Excitation Spectroscopy in Even $5p^5(^2P_{1/2})nl'$ $[K']_J$ (l'=1, 3) Autoionizing Resonances of Xe

Chun-yan Li[a*], Ting-ting Wang[b], Jun-feng Zhen[b], Yang Chen[b*], Zhi-wei He[a]

a. College of Science, China Agricultural University, Beijing 100083, China
b. Hefei National Laboratory for Physical Sciences at the Microscale and Department of Chemical Physics, University of Science and Technology of China, Hefei 230026, China

(Dated: Received on April 10, 2013; Accepted on May 27, 2013)

The even-parity autoionizing resonance series $5p^5np'$ $[3/2]_1$, $[1/2]_1$, and $5p^5nf'$ $[5/2]_3$ of xenon have been investigated, excited from the two metastable states $5p^56s$ $[3/2]_2$ and $5p^56s'$ $[1/2]_0$ in the photon energy range of 28000−42000 cm^{-1} with experimental bandwidth of $\sim$0.1 cm^{-1}. The excitation spectra of the even-parity autoionizing resonance series show typical asymmetric line shapes. New level energies, quantum defects, line profile indices and resonance widths, resonance lifetimes and reduced widths of the autoionizing resonances are derived by a Fano-type line-shape analysis. The line profile index and the resonance width are shown to be approximately proportional to the effective principal quantum number. The line separation of the $5p^5np'$ autoionizing resonances is discussed.

Key words: Xenon, Autoionizing resonance, Fano-type lineshape

I. INTRODUCTION

The high Rydberg states of rare gases have been a subject of interest to spectroscopists for many years. Especially the autoionizing resonance state (ARS) is attractive for experimental and theoretical studies because they are rather isolated and their characteristics can be determined with high accuracy [1, 2]. The energy of the Rydberg electron is very sensitive to the potential associated with the ion core and provides information on the polarizability of the many-electron core. The width of the ARS is determined by the interaction of the excited states with the continuum and the nearby ARS of the same parity and total angular momentum J; these interactions are strongly affected by many-electron correlations. Therefore, studies of ARS allow us to obtain deeper insight into intra-atomic electron dynamics, and a critical comparison between the measured and calculated characteristics of the ARS can provide a crucial test of the theoretical approach. The rare gases (except helium) possess two relatively closely spaced ionization limits corresponding to the $^2P_{3/2}$ and $^2P_{1/2}$ states of the ion core, with the Rydberg series converging to each of these two limits. The high-lying Rydberg states of rare gas atoms, especially the autoionizing states between the two ionization limits, have been of long-standing interest to spectroscopists. Compared to other nonradiative rare gas atoms, Xe has an atomic core of the largest mass number, which implies that its Rydberg electron lies the highest in the atomic shell. Therefore the studies on the high-lying autoionizing Rydberg states of Xe may provide deeper insights into the configurations of these states and shine light on other multi-electron atomic systems as well.

Since the ionization limits and the autoionizing Rydberg states of the rare gas atoms are of high energies, the spectroscopic investigations starting from their ground states usually necessitate vacuum ultraviolet (VUV) radiation, which makes their high resolution spectra hard to obtain. Promoting one of the 5p-subshell electrons of Xe to its 6s orbital yields four levels attributable to such configurations as $5p^56s$ $[3/2]_{1,2}$ and $5p^56s'$ $[1/2]_{0,1}$. The $5p^56s$ $[3/2]_1$ and $5p^56s'$ $[1/2]_1$ levels quickly decay radiatively to the ground state, while the $5p^56s$ $[3/2]_2$ and $5p^56s'$ $[1/2]_0$ levels are metastable with the predicted lifetimes being 149.5 s and 78.2 ms respectively [3], and the energy positions being at 67067.54 and 76196.78 cm^{-1} relative to the ground state respectively [4]. These metastable levels facilitate access to the high-lying Rydberg levels by means of single-photon (UV) or two-photon (visible) excitation spectroscopy, a goal that is usually hard to achieve via a direct VUV photon excitation starting from the ground state, partly because of the transition selection rules. More importantly, the excitation spectra can thus be obtained with a narrow-linewidth laser source, thereby ensuring high resolution.

The spectroscopy of high Rydberg states of Xe, especially the autoionizing states, has been extensively investigated [4−19]. However, the studies on the even-parity autoionizing Rydberg states of Xe remain un-

*Authors to whom correspondence should be addressed. E-mail: chunyanl@cau.edu.cn, yangchen@ustc.edu.cn

systematic, and the resolution of the obtained spectra is relatively low [5−16]. In 1958, Thekaekara and Dieke first observed some $5p^5nf'$ (n=4−8) autoionizing states excited from intermediate state $5p^55d$ [5], but the measurement was so inaccurate. Rundel *et al.* reported the excitation spectra of single photon excitation to the even parity autoionizing states $5p^5(^2P_{1/2})np'$ (n=7, 8) and $5p^5(^2P_{1/2})nf'$ (n=4, 5) from the second metastable level $5p^56s'\ [1/2]_0$ [6], and analyzed the spectra using the line-shape formula derived by Fano. Later Grandin and Husson reported the level energies of $5p^57p'$ ($[3/2]_{1,2}$ and $[1/2]_{0,1}$) and $5p^5nf'\ [5/2]_2$ (n=4, 5) autoionizing resonances [7]. Knight and Wang studied the autoionizing resonance series $5p^5np'\ [3/2]_1$, $[1/2]_1$ (n=7−17) excited from the second metastable level $5p^56s'\ [1/2]_0$, and reported the corresponding level energies, quantum defects and resonance widths [8]. Blazewicz *et al.* studied the $5p^5np'$ (n=10, 11) $[5/2]_2$, $[1/2]_0$ and $5p^5nf'$ (n=4−11) autoionizing resonances via four-photon excited from the ground state, reported the corresponding level energies and quantum defects [9]. In the end of the last century ten years, Higgin *et al.* reported the resonance widths of $5p^54f'\ [7/2]_{3,4}$, $[5/2]_{2,3}$ excited from $5p^55d\ [3/2]_2$ [10]. Koeckhoven *et al.* obtained the spectra of $5p^5nf'\ [7/2]_4$, $[5/2]_2$ (n=4−12) and $5p^5np'\ [3/2]_1$, $[1/2]_0$ (n=8−13) from the ground state via four-photon excitation, then analyzed the line shapes of the part resonances using a line-shape formula derived by Ueda [11]. Kau *et al.* observed excitation spectra of $5p^57p'\ [3/2]_1$, $[1/2]_1$ from $5p^56s'\ [1/2]_0$ and reported the level energies, resonance widths and line profile indices [12]. Gisselbrecht *et al.* employed synchrotron radiation to excite $5p^55d\ [3/2]_1$ and $5p^56d\ [3/2]_1$ to autoionizing resonances series $5p^5nf'\ [5/2]_2$ (n=4, 7−13) [13], then analyzed the line shapes of the part resonances (n=4, 7−9) using Fano lineshape formula, the corresponding line profile index q and resonance width Γ were obtained. Hanif and his research team investigated the spectra of $5p^57p'$, $5p^54f'$ and $5p^55f'$ excited from the $5p^56s'\ [1/2]_{0,1}$, and $5p^55d$ respectively, then determined the resonance energies, quantum defects, line-shape parameters and resonance widths by fitting the observed resonance profiles using Fano's formula for the photoionization cross section [14]. Meyer *et al.* studied $5p^511p'$, $5p^54f'$, $5p^57f'$ and $5p^58f'$ autoionizing resonances with synchrotron radiation, carried out the calculations of the observed experimental parameters using a configuration interaction Pauli-Fock approach with inclusion of core polarization [15]. Peter and his coworkers reported the experimental investigation of the autoionizing resonances $14p'\ [1/2]_1$, $[3/2]_{1,2}$ at bandwidths about 0.25 cm^{-1}, the level energies (quantum defects) and widths for these resonances have been derived by a Fano-type lineshape analysis, thus yielding reduced resonance widths [16].

The odd-parity autoionizing states of Xe have mainly been studied [4, 17−19] by means of a VUV laser multiphoton excitation or a synchronization radiation of Xe from its ground state to the target states of interest. In 1990, Wu *et al.* measured the photoionization cross sections and photoelectron angular parameters of the $5p^5(^2P_{1/2})\ 8s'$, $6d'$ autoionization resonances for Xe with photon resolution widths as low as 0.23 cm^{-1} by means of synchrotron-based photoelectron spectroscopy [17]. Koeckhoven *et al.* obtained the spectra of $5p^5ns'\ [1/2]_1$ (n=8−30), $5p^5nd'\ [3/2]_1$ (n=10−15), $5p^5nd'\ [5/2]_3$ (n=8−29), and $5p^5ng'\ [7/2]_3$ (n=5−20) from the ground state via three-photon excitation, then analyzed the line shapes of the part resonances using a line-shape formula derived by Ueda and obtained the corresponding line profile parameters q, quantum defects and widths parameters [18]. In 2002, Petrov *et al.* carried out calculations of the resonance widths for all $5p^520l'\ [K]_J$ series with l'=0−5 within the single-electron Pauli-Fock approach [19]. Hanif *et al.* measured the $5p^5nd'$ (n=7−9) $[5/2]_{2,3}$, $[3/2]_2$ autoionizing resonances of Xe by means of two-step resonant laser excitation from the metastable Xe (J=2, 0) levels, level energies and resonance widths have been derived by a Fano-type lineshape analysis [4].

Although many experiments have been done for the Xe autoionizing Rydberg states including $5p^5np'$ and $5p^5nf'$, there are few high-resolution spectroscopic studies and very few line profile parameters available. We recently reported the systematic experiment study of the autoionizing $5p^5np'$ and $5p^5nf'$ resonance series of Xe by using pulsed DC discharge along with single UV photon excitation and the TOF-MS technique [20]. In that work, the metastable Xe^* ($5p^56s\ [3/2]_2$ and $5p^56s'\ [1/2]_0$) atoms are produced by a pulsed high-voltage DC discharge. Starting from these metastable states, the high resolution excitation spectra pertinent to the autoionizing Rydberg states $5p^5np'\ [3/2]_1$, $[1/2]_1$, and $5p^5nf'\ [5/2]_3$ of Xe were readily obtained via a subsequent narrow-linewidth (<0.1 cm^{-1}) UV laser excitation. These autoionizing resonance states subsequently decay to Xe^+ ions, which are detected using the time-of-flight (TOF) mass spectrometry. The excitation spectra of the autoionizing resonance series are recorded in the form of the Xe^+ ion intensities as a function of excitation UV laser radiation. The high-resolution excitation spectra show typical asymmetric line shapes. In present work, the high-resolution excitation spectra are fitted using Fano line-shape formula, and new results for the resonance energies, quantum defects, line profile indices, resonance widths, resonance lifetimes, and reduced widths are derived from the observed resonance spectra.

II. EXPERIMENTS

The experiment was conducted in a laser ionization mass spectrometer described previously [20]. Briefly, the photoionization experimental apparatus includes the metastable Xe^* atoms source and the ion detec-

DOI:10.1063/1674-0068/26/04/374-380

tion system. The metastable Xe* atoms were produced by a DC discharge of a mixture of a gas mixture of 10%Xe and 90%Ar at a stagnation pressure of ∼5 atm. A pulsed high voltage of about 2 kV was supplied to the electrodes producing a discharge in the area of the orifices of the copper electrodes. The supersonic beam after the DC discharge was collimated by a 3 mm diameter skimmer and entered into the photoexcitation and photoionization chamber. The photoionization chamber was maintained at typical pressures of ∼0.1 and <0.01 mPa, respectively, with and without the operation of the beam. A Nd:YAG laser (Spectra Physics, GCR-190) pumping a dye laser (Lumonics, HT-500) was used as the light source. The dye laser output was frequency doubled with a second harmonic generator (Lumonics, HT-1000) (pulse duration of UV radiation is about 8 ns, energy per UV pulse is typically 50 μJ) and then focused perpendicularly on the metastable Xe* beam by a 250 mm focal length lens. Ions generated via autoionizing process at the ionization zone were introduced and accelerated to the flight tube of the TOF mass spectrometer and then detected by micro-channel plates (MCP). The mass resolved ion signal from the MCP was amplified by an amplifier (Stanford Research System, SR445) and averaged by a digital oscilloscope (Tektronix, TDS3032B) or a computer data acquisition system. A multi-channel delay pulsed generator was used to control the relative time delays among the nozzle, the laser, and the DC discharge.

The excitation spectra were obtained by mass selectively recording the Xe^+ ion (m/z=124, 126, 128, 129, 130, 131, 132, 134, 136) signal as a function of the laser wavelength. No attempt was made to normalize the ion signal intensity against the laser power. The typical scanning speed of the dye laser was 0.001 nm/s at a 10 Hz laser repetition. Calibration of the laser wavelength was achieved by a wavelength meter (Coherent, WaveMaster 33-2650).

III. RESULTS AND DISCUSSION

The excited levels of the rare gas are designated in the $j_c l[K]_J$ coupling scheme [8, 21−23], in which the orbital angular momentum l of the excited electron is weakly coupled to the total angular momentum j_c (3/2 or 1/2) of the $np^5_{j_c}$ ionic core to yield the resultant quantum angular momentum K. K is then weakly coupled with the spin s of the excited electron giving total angular momentum J. The propensity rules for electric dipole transitions in the jK-coupling scheme are: ΔJ=0, ±1, ΔK=0, ±1, and Δj=0. These rules are well observed, and wherever ΔJ=ΔK=+Δl, the transition lines possess higher intensity. However, the Δj=0 rule is not followed strictly, since transitions with a change of the ionic core are also often observed.

Since the first adiabatic ionization potential of Xe is 97833.79 cm^{-1}, only one photon in the energy range of 28000−42000 cm^{-1} used in the work is required to excite the two aforementioned Xe* metastable states to the autoionizing states of interest. There are many natural isotopes of Xe, the ^{129}Xe was mass selected as the target in the present study because of its highest isotopic abundance. Based on the transition rules and the threshold for direct photoionization from the Xe* metastable to the autoionizing resonance series, the observed series of the autoionizing structures as reported in our previous paper [20] are identified as being due to the following equation respectively,

$$5p^5(^2P_{1/2})6s'\ [1/2]_0 \xrightarrow{h\nu} 5p^5(^2P_{1/2})np'\ [3/2]_1, [1/2]_1 \quad (1)$$

$$5p^5(^2P_{3/2})6s\ [3/2]_2 \xrightarrow{h\nu} 5p^5(^2P_{1/2})np'\ [3/2]_1, [1/2]_1 \quad (2)$$

$$5p^5(^2P_{3/2})6s\ [3/2]_2 \xrightarrow{h\nu} 5p^5(^2P_{1/2})nf'\ [5/2]_3 \quad (3)$$

Since the autoionizing resonances lie between the two ionization potentials in the $^2P_{3/2}$ continuum, the perturbation arising from interactions among the resonance series having the same parity and J, and the perturbation arising from interactions with the $^2P_{3/2}$ continuum, are complex. The perturbation influences the Rydberg electron of Xe and manifests on the variation of the principal quantum defects. The width of the spectrum peak reflects the lifetime of the resonance. The experimental results show that, as the principal quantum number n increases, the quantum defects of the given series increase whereas the widths of the autoionizing peaks corresponding to the given series decrease. This is expected because the interaction with the $^2P_{3/2}$ continuum is greater near the second ionization threshold. The lifetime of the autoionizing resonances will be discussed below.

A. Line-profile analysis of the $5p^5np'$ and $5p^5nf'$ autoionizing resonances

The line profiles for all the observed transitions between 28000 and 42000 cm^{-1}, show typical asymmetric line shapes, as seen in Fig.1. A theoretical treatment of these line shapes due to autoionizing transitions has been carried out by Fano [24, 25]. For an isolated autoionizing state, the photoion production cross section can be described by the Fano formula:

$$\sigma(E) = \sigma_b + \sigma_a \frac{(q+\varepsilon)^2}{1+\varepsilon^2} \quad (4)$$

$$\varepsilon = \frac{E - E_r}{\Gamma/2} \quad (5)$$

here σ_b represents the portion of the cross section describing transitions to the continuum that do not interact with the quasi-bound (autoionizing) states, and σ_a is the resonant portion of the cross section. E is the

DOI:10.1063/1674-0068/26/04/374-380

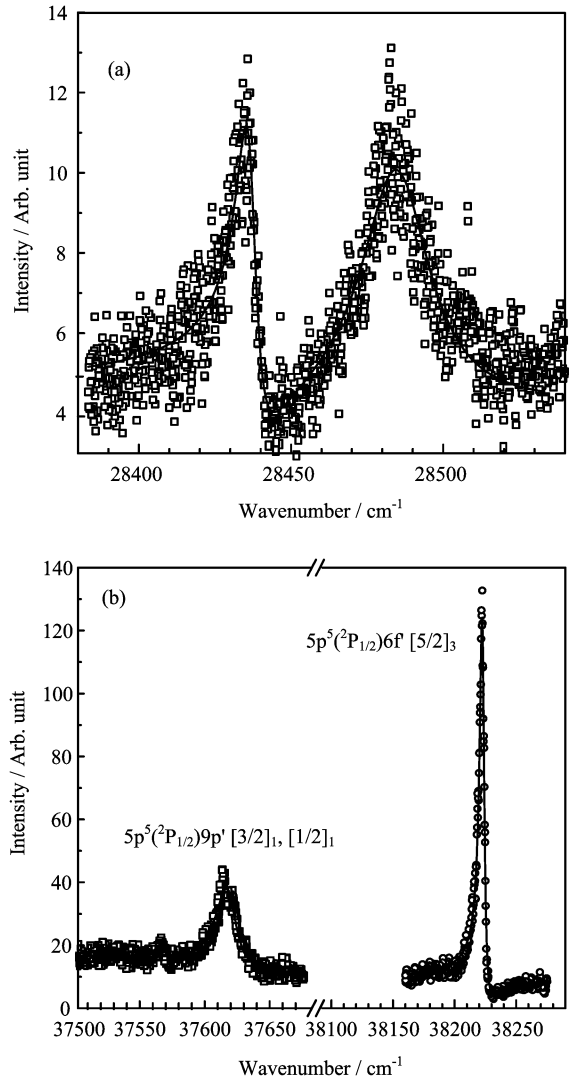

FIG. 1 The partially expanded spectra of the autoionizing resonances. The smooth curves represent fits to the experimental spectra (dots). (a) The experimental data and Fano line profile fitting curve of autoionizing line $5p^59p'$ $[3/2]_1$, $[1/2]_1$ excited from $5p^56s'$ $[1/2]_0$. (b) The experimental data and Fano line profile fitting curve of autoionizing lines $5p^59p'$ $[3/2]_1$, $[1/2]_1$, and $5p^56f'$ $[5/2]_3$ excited from $5p^56s$ $[3/2]_2$.

observed term energy, E_r is the resonance energy, q is the line profile index, and Γ is the resonance width.

Fano profile has been fitted to the present data, providing values of E_r, q, Γ for each of the observed transitions (listed in Tables I–IV). The partially expanded spectra of the autoionizing resonances are shown in Fig.1 as the example to illustrate the comparison of the Fano profile curve fits to the experimental spectra. Figure 1(a) shows the experimental data and Fano line profile fitting curve of the autoionizing line $5p^59p'$ $[3/2]_1$, $[1/2]_1$ excited from the metastable level $5p^56s'$ $[1/2]_0$. Figure 1(b) shows the experimental data and Fano line profile fitting curve of the autoionizing lines $5p^59p'$ $[3/2]_1$, $[1/2]_1$ and $5p^56f'$ $[5/2]_3$ excited from the first metastable level $5p^56s$ $[3/2]_2$. Note that most of the line profile analysis of the $5p^5np'$ $[3/2]_1$, $[1/2]_1$ and $5p^5nf'$ $[5/2]_3$ autoionizing resonances are reported for the first time. For members of a Rydberg series, the reduced width Γ_r is defined as $\Gamma_r=\Gamma_n(n^*)^3$, where $n^*=n-\delta$ is the effective quantum number, and the corresponding quantum defect δ and effective quantum number n^* are calculated using the Rydberg formula. The obtained values of the reduced width Γ_r are listed in Tables I–IV. The lifetime of the upper state against autoionization τ is readily determined from $\tau=\hbar/\Gamma$, and the values of τ are also included in Tables I–IV.

As shown from the data listed in the tables, the absolute value of line profile index q decreases when n increases (np' autoionizing resonances series have lager error for superposition of the three states). This indicates that the profile symmetry for high autoionizing resonances is more asymmetric, *i.e.*, the portion of the cross section describing transition to the continuum possesses more percentage in the transition from the lower electronic level to higher upper autoionizing resonances. The present results show that the resonance width Γ value decreases as the principal quantum number n increases, which directly reflects the decrease in natural linewidths of the np' and nf' resonances and increase of their lifetimes. This is expected because the interaction of the resonance states with the $^2P_{3/2}$ continuum is greater (thus faster autoionization) when the resonances are near the threshold, where the density of the continuum is higher. The lifetimes of the $5p^5np'$

TABLE I Parameters obtained by line profile analysis for the $5p^5np'$ $[3/2]_1$←$6s'$ $[1/2]_0$. E_r^*, Γ, and Γ_r in cm^{-1}. τ in ps.

n	E_r^*	q	Γ	τ	δ	Γ_r
9	104633.78	−2.14±0.05	7.69±0.29	0.69	3.581	1224
10	105710.58	−1.67±0.05	5.21±0.26	1.02	3.577	1381
11	106380.78	−1.32±0.10	2.53±0.39	2.10	3.574	1036
12	106825.58	−1.41±0.10	1.64±0.22	3.24	3.573	981

* E_r is the $5p^5np'$ $[3/2]_1$ states' resonance energy excited from $6s'$ $[1/2]_0$ (76196.78 cm^{-1}).

TABLE II Parameters obtained by line profile analysis for the $5p^5np'$ $[1/2]_1$←$6s'$ $[1/2]_0$. E_r^*, Γ, and Γ_r in cm^{-1}. τ in ps.

n	E_r^*	q	Γ	τ	δ	Γ_r
9	104681.78	−18.51±2.29	27.04±0.90	0.19	3.546	4387
10	105739.28	−5.64±0.38	11.31±0.60	0.46	3.542	3046
11	106399.78	−4.73±0.14	7.58±0.87	0.69	3.538	3149
12	106838.58	−4.32±0.13	5.28±0.51	0.99	3.537	3200

* E_r is the $5p^5np'$ $[1/2]_1$ states' resonance energy excited from $6s'$ $[1/2]_1$ (76196.78 cm^{-1}).

DOI:10.1063/1674-0068/26/04/374-380

TABLE III Parameters obtained by line profile analysis for the $5p^5np'$ $[3/2]_1$←6s $[3/2]_2$ and $5p^5np'$ $[1/2]_1$←6s $[3/2]_2$. E_r^*, Γ, and Γ_r in cm^{-1}. τ in ps.

n	$5p^5np'$ $[3/2]_1$←6s $[3/2]_2$						$5p^5np'$ $[1/2]_1$←6s $[3/2]_2$					
	E_r^*	q	Γ	τ	δ	Γ_r	E_r^*	q	Γ	τ	δ	Γ_r
7	98849.54	−4.06±0.24	36.53±2.10	0.15	3.605	1429	99075.54	−6.77±0.22	121.52±2.67	0.04	3.564	4930
			51±30[a]		3.5994[a]				88.6±1[a]		3.5665[a]	
			28.8±0.5[b]		3.6042[b]				76.8±0.5[b]		3.5670[b]	
			30±2[c]		3.604[c]				75±2[c]		3.568[c]	
			29.7±3[d]						73.1±6[d]			
			28±3[e]						61±8[e]			
8	102757.54	−1.25±0.10	16.40±2.69	0.32	3.579	1417	102823.54	−7.88±0.19	46.44±0.84	0.11	3.552	4087
			13.4±0.5[b]		3.5910[a]				37.0±0.5[a]		3.5519[a]	
									31.2±0.5[b]		3.5522[b]	
9	104634.54	−2.02±0.18	8.81±1.25	0.60	3.581	1402	104683.54	−5.13±0.15	19.03±0.48	0.28	3.545	3089
10	105709.54	−2.17±0.33	4.93±1.16	1.08	3.579	1305	105740.04	−6.48±0.36	12.73±0.50	0.42	3.541	3430
11	106380.24	−3.49±0.69	3.72±0.79	1.43	3.575	1523	106399.04	−7.88±0.77	6.74±0.36	0.79	3.54	2798
12	106825.54	−2.49±0.54	1.82±0.54	2.92	3.573	1089	106838.34	−4.64±0.20	5.35±0.21	0.99	3.538	3242
13	107135.34	−2.07±0.54	0.92±0.37	5.77	3.575	770	107145.34	−4.29±0.23	3.57±0.20	1.49	3.537	3025
14	107361.74	−2.53±0.62	0.95±0.32	5.59	3.572	1077	107368.14	−7.90±0.97	2.79±0.19	1.90	3.538	3195
15	107530.84	−3.00±1.36	0.71±0.39	7.48	3.570	1060	107535.84	−6.12±0.72	2.52±0.20	2.11	3.536	3797
16	107660.54	−2.09±0.87	0.59±0.34	9.00	3.570	1133	107664.24	−5.39±0.63	2.06±0.18	2.58	3.538	3987
17	107761.94	−0.79±0.17	0.33±0.28	16.09	3.575	798	107764.94	−3.81±0.34	1.44±0.13	3.69	3.542	3510
18	107842.84	−6.69±4.58	0.59±0.27	9.00	3.583	1768	107845.54	−11.19±0.92	0.92±0.09	5.77	3.546	2778

[*] E_r is the states' resonance energy excited from 6s $[3/2]_2$ (67067.54 cm^{-1}).
[a] Experimental results from 6s $[3/2]_2$ [6].
[b] Experimental results from 6s′ $[1/2]_0$ [6].
[c] Experimental results from 6s′ $[1/2]_0$ [14].
[d] Experimental results from 6s′ $[1/2]_0$ [12].
[e] Experimental results from 6s′ $[1/2]_0$ [8].

TABLE IV Parameters obtained by line profile analysis for the $5p^5nf'$ $[5/2]_3$←6s $[3/2]_2$. E_r^*, Γ, and Γ_r in cm^{-1}. τ in ps.

n	E_r^*	q	Γ	τ	δ	Γ_r	n	E_r^*	q	Γ	τ	δ	Γ_r
4	101426.14	−8.61±0.23	5.78±0.08	0.92	0.025	363	9	107005.44	−3.90±0.07	2.15±0.04	2.47	0.035	1551
			7.6±0.5[a]		0.0259[a]					0.9±0.8[c]			
			4.0±0.5[b]				10	107265.54	−4.92±0.13	1.57±0.03	3.38	0.036	1556
			3.3±0.3[c]				11	107457.99	−6.60±0.30	1.26±0.03	4.21	0.036	1667
			7.1±0.2[d]				12	107604.02	−6.75±0.33	1.16±0.03	4.58	0.037	1980
5	103929.44	−7.08±0.15	6.39±0.08	0.83	0.029	785	13	107717.02	−12.10±1.05	0.96±0.03	5.53	0.045	2078
			5.2±0.5[a]		0.0281[a]		14	107807.07	−9.19±0.72	0.83±0.03	6.40	0.048	2255
			7.1±0.2[d]				15	107879.69	−12.41±1.39	0.79±0.03	6.72	0.052	2627
6	105290.34	−4.21±0.05	4.95±0.06	1.07	0.031	1053	16	107939.26	−13.49±2.04	0.77±0.03	6.89	0.054	3105
7	106109.54	−5.16±0.11	3.19±0.06	1.66	0.034	1077	17	107988.52	−11.53±1.88	0.77±0.04	6.89	0.058	3756
			1.1±0.6[c]				18	108029.99	−13.88±2.86	0.85±0.05	6.25	0.056	4894
8	106640.94	−3.95±0.05	2.60±0.03	2.04	0.035	1314	19	108065.09	−7.88±1.08	0.69±0.05	7.69	0.054	4714
			0.9±0.7[c]				20	108094.69	−7.79±1.53	0.60±0.06	8.85	0.065	4789
							21	108120.34	−7.02±2.56	0.53±0.11	10.02	0.069	4889

[*] E_r is the $5p^5np'$ $[3/2]_1$ states' resonance energy excited from 6s $[3/2]_2$ (67067.54 cm^{-1}).
[a] Experimental results from 6s $[3/2]_2$ [6].
[b] Experimental results from 5d $[5/2]_2$ [14].
[c] Experimental results from 6d $[3/3]_2$ $[1/2]_0$ [13].
[d] Experimental results from 5d $[3/2]_2$.

DOI:10.1063/1674-0068/26/04/374-380

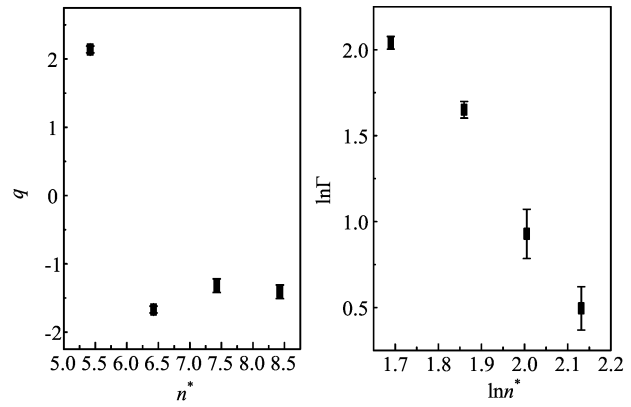

FIG. 2 Autoionizing line profile index q and resonance width Γ of the $5p^5np'\ [3/2]_1$ series excited from $6s'\ [1/2]_0$ plotted against effective quantum number n^*.

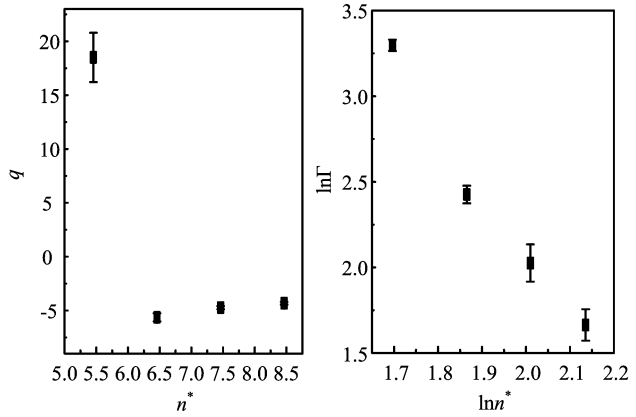

FIG. 3 Autoionizing line profile index q and resonance width Γ of the $5p^5np'\ [1/2]_1$ series excited from $6s'\ [1/2]_0$ plotted against effective quantum number n^*.

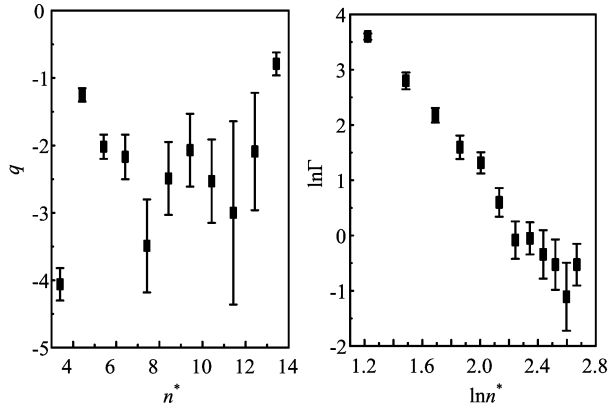

FIG. 4 Autoionizing line profile index q and resonance width Γ of the $5p^5np'\ [3/2]_1$ series excited from 6s $[3/2]_2$ plotted against effective quantum number n^*.

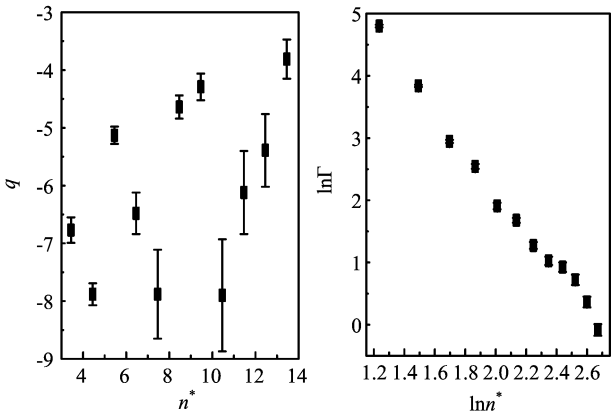

FIG. 5 Autoionizing line profile index q and resonance width Γ of the $5p^5np'\ [1/2]_1$ series excited from 6s $[3/2]_2$ plotted against effective quantum number n^*.

$[3/2]_1$ and $[1/2]_1$ autoionizing resonance series change significantly with a ratio ∼100 between the observed highest and lowest levels, whereas the lifetimes of the $5p^5nf'\ [5/2]_3$ change with a ratio ∼10.

It is noted that the q and Γ value varies with the effective quantum number n. In order to see the relations for q and Γ value *vs.* n^*, q and Γ as a function of n^* are plotted and shown in Fig.2−Fig.6. From these figures, the empirical results are obtained: q is proportional to n^* for the autoionizing resonance series roughly, and $\ln\Gamma$ is approximately proportional to $\ln n^*$.

B. Line separation of the $5p^5np'$ autoionizing resonances

Because in the jK coupling scheme, the energy difference depends only on the Slater exchange integral G^1 resulting from the electrostatic interaction, the fine structure interval is expected to be proportional to $1/(n^*)^3$ [8, 26]. The experimental fine structure interval data of the $5p^5np'$ autoionizing resonances are plotted as a function of n^* as $\ln n^*$ and shown in Fig.7. The line has a slope of -3.009 ± 0.076 (difference between between $5p^5np'\ [1/2]_1$ and $5p^5np'\ [3/2]_1$), comparable to the expected slope of -3. The results are in good agreement with the theoretical estimate of the fine structure interval.

IV. CONCLUSION

We have carried out the experiment study of the autoionizing $5p^5np'$ and $5p^5nf'$ resonance series of Xe by using pulsed DC discharge along with single UV photon excitation and the TOF-MS technique. The Fano line profile analysis of the excitation spectra is carried out and the Fano parameters of the systematic autoionizing series are reported. The line profile index q and resonance width Γ are shown to be approximately proportional to the effective principal quantum number n^*. The line separation of the $5p^5np'$ autoionizing resonances is also discussed.

DOI:10.1063/1674-0068/26/04/374-380

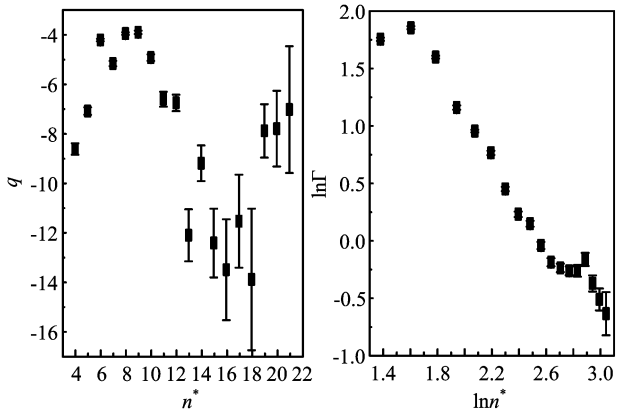

FIG. 6 Autoionizing line profile index q and resonance width Γ of the $5p^5nf'$ $[5/2]_3$ series excited from 6s $[3/2]_2$ plotted against effective quantum number n^*.

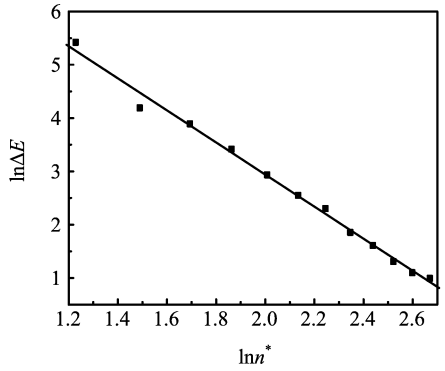

FIG. 7 Energy difference of the $5p^5np'$autoionizing resonances energy levels plotted against $\ln n^*$. The slope is -3.009 ± 0.076 for the difference of $5p^5np'$ $[1/2]_1$ and $5p^5np'$ $[3/2]_1$.

V. ACKNOWLEDGEMENTS

This work is supported by the National Natural Science Foundation of China (No.51007092).

[1] K. Z. Xu, *Advanced Atomic and Molecular Physics*, Beijing: Science Press, 4 (2000).
[2] T. X. Lu and Y. Q. Lu, *Principles and Applications of Laser Spectroscopic Techniques*, Hefei: University of Science and Technology of China Press, 368 (1999).
[3] N. E. Small-Warren and L. Y. Chow Chiu, Phy. Rev. A **11**, 1777 (1975).
[4] M. Hanif, M. Aslam, R. Ali, S. A. Bhatti, M. A. Baig, D. Klar, M. W. Ruf, I. D. Petrov, V. L. Sukhorukov, and H. Hotop, J. Phys. B **37**, 1987 (2004).
[5] M. Thekaekara and G. H. Dieke, Phys. Rev. **109**, 2029 (1958).
[6] R. D. Rundel, F. B. Dunning, H. C. Jr. Goldwire, and R. F. Stebbing, J. Opt. Soc. Am. **65**, 628 (1975).
[7] J. P Grandin and X. Husson, J. Phys. B **14**, 433 (1981).
[8] R. D. Knight and L. G. Wang, J. Opt. Soc. Am. B **3**, 1673 (1986).
[9] P. R. Blazewicz, J. A. D. Stockdale, J. C. Miller, T Efthimipoulos, and C. Fotakis, Phys. Rev. A **35**, 1092 (1987).
[10] M. J. Higgins and C. J. Latimer, Phys. Scr. **48**, 675 (1993).
[11] S. M. Koeckhoven, W. J. Burma, and C. A. de Lange, Phys. Rev. A **51**, 1097 (1995).
[12] R. Kau, D. Klar, S. Schohl, S. Baier, and H. Hotop, Z. Phys. D **36**, 23 (1996).
[13] M. Gisselbrecht, A. Marquette, and M. Meyer, J. Phys. B **31**, L977 (1998).
[14] M. Hanif, M. Aslam, M. Riaz, S. A. Bhatti, and M. A. Baig, J. Phys. B **38**, S65 (2005).
[15] M. Meyer, M. Gisselbrecht, A. Marquette, C. Delisle, M. Larzilliere, I. D. Petrov, N. V. Demekhina, and V. L. Sukhorukov, J. Phys. B **38**, 285 (2005).
[16] T. Peter, T. Halfmann, U. Even, A. Wunnenberg, I. D. Petrov,V. L. Sukhorukov, and H. Hoptop, J. Phys. B **38**, S51 (2005).
[17] J. Z. Wu, S. B. Whitfield, C. D. Caldwell, M. O. Krause, P. van der Meulen, and A. Fahlman, Phys. Rev. A **42**, 1350 (1990).
[18] S. M. Koeckhoven, W. J. Burma, and C. A. de Lange, Phys. Rev. A **49**, 3322 (1994).
[19] I. D. Petrov, V. L. Sukhorukov, and H. Hotop, J. Phys. B **35**, 323 (2002).
[20] C. Y. Li, T. T. Wang, J. F. Zhen, Q. Zhang, and Y. Chen, Chin. J. Chem. Phys. **21**, 401 (2008).
[21] G. Racah, Phys. Rev. **62**, 438 (1942).
[22] I. I. Sobelman, *Atomic Spectra and Radiative Transitions*, Berlin Heidelberg: Springer-Verlag (1979).
[23] R. D. Cowan, *The Theory of Atomic Structure and Spectra*, Berkley: University of California Press, (1981).
[24] U. Fano, Phys. Rev. **124**, 1866 (1961).
[25] U. Fano and J. W. Cooper, Phys. Rev. **137**, A1364 (1965).
[26] J. M. Weber, K. Ueda, D. Klar, J. Kreil, M. W. Ruf, and H. Hotop, J. Phys. B **32**, 2381 (1999).

DOI:10.1063/1674-0068/26/04/374-380